Article

Difunctionalization of bicyclo[1.1.0]butanes enabled by merging C−C cleavage and ruthenium-catalysed remote C−H activation

Shan Chen, Zhimin Xu, Binbin Yuan, Xue-Ya Gou & Lutz Ackermann ✉

The high fraction of sp^3-hybridized carbon atom (Fsp^3) character of cyclobutane derivatives renders them as highly promising bioisosteres for otherwise typically flat arenes. Here, to address the current needs in medicinal chemistry for Fsp^3-rich molecules, we disclose a distinct strategy that exploits the merger of C−C scission in bicyclo[1.1.0]butanes (BCBs) with ruthenium-catalysed remote C−H functionalization of heteroarenes, affording densely substituted cyclobutanes in a chemo-controlled manner. This approach enabled the rapid and efficient synthesis of versatile tri- and tetrasubstituted cyclobutanes by coupling a wide range of mono- or disubstituted BCBs with heteroarenes and alkyl halides under mild reaction conditions, featuring ample substrate scope. The C−C/C−H functionalization was ensured by a multifunctional ruthenium(II) catalyst that enabled ruthenacycle-mediated halogen-atom transfer (Ru-XAT), as well as the selective functionalization of BCBs by strain release. Experimental and computational mechanistic studies unravelled a multi-catalysis manifold, while the C−H/C−C functionalization strategy allowed for telescoping late-stage modification.

In the quest of 'escaping from flatland'[1–8], highly functionalized cyclobutanes with unique puckered linear geometry have received increasing attention in medicinal chemistry. The fraction of sp^3-hybridized carbon atoms (Fsp^3) was identified as a key descriptor of drug likeness, and the increased Fsp^3 in cyclobutanes renders them as a privileged motif for isosteres in drug design[9]. The incorporation of cyclobutane scaffolds often enhances the physicochemical and pharmacokinetic properties of drug molecules. In contrast to usually flat arene rings, polysubstituted cyclobutanes with high Fsp^3 can provide, among others, improved solubility due to their nonplanar substituent vectors. Indeed, several pharmaceuticals featuring 1,3-bifunctional cyclobutanes have been clinically tested, such as PF-03654746 (ref. 10), NVP-ADW 742 (ref. 11), NK1 selective antagonists[12] and Linsitinib[13], translating into a strong need for innovative cyclobutane syntheses (Fig. 1a). However, in contrast to rather well-established bifunctionalization of bicyclo[1.1.0]pentanes (BCPs)[14–18] and ring

expansions of bicyclo[1.1.0]butanes (BCBs)[19–41] (Fig. 1b), strategies to access structurally complex cyclobutanes are, unfortunately, scarce. Thus far, these syntheses are limited to radical or nucleophilic additions to BCBs, typically resulting in mono- or disubstituted cyclobutanes[42–49], with only few examples for densely substituted cyclobutanes[50–54]. Furthermore, the aforementioned transformations are largely limited to rather harsh conditions and elements of prefunctionalization on the coupling partner, while the merger of C−C activations[55–60] of BCBs with remote C−H activation[61] has thus far proven elusive. To address these current topical needs, we have now developed the merger of BCBs C−C functionalization with remote C−H functionalization[62–73] by a single, yet powerful, ruthenium(II) catalyst. Salient features of our findings include (1) versatile 1,3-difunctionalization of BCBs for tri- and tetrasubstituted Fsp^3-rich cyclobutanes; (2) a single ruthenium complex for a multi-catalysis manifold including an efficient ruthenacycle-mediated halogen-atom transfer (Ru-XAT) process, C−C scission and *meta*-C−H

Wöhler-Research Institute for Sustainable Chemistry, Georg-August-Universität Göttingen, Göttingen, Germany.
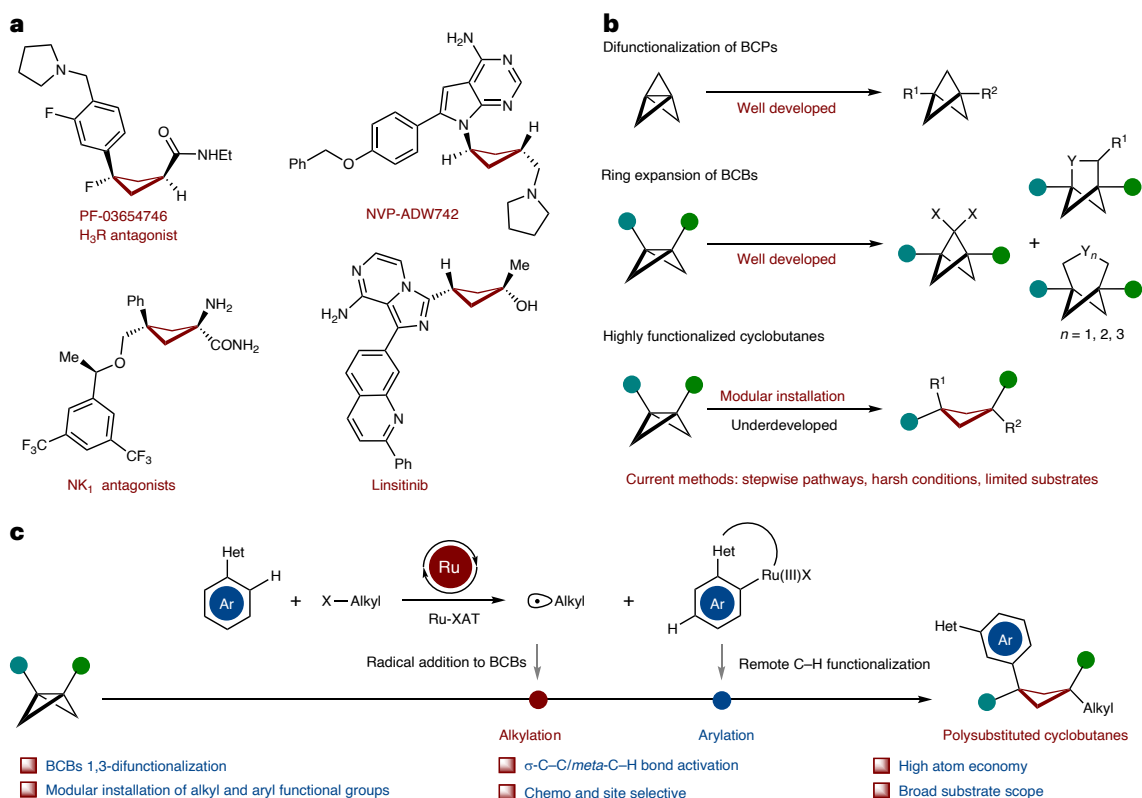✉e-mail: Lutz.Ackermann@chemie.uni-goettingen.de

Fig. 1 | Design blueprint for the difunctionalization of BCBs to access 1,1,3-trisubstituted and 1,1,3,3-tetrasubstituted cyclobutanes enabled by remote C–H activation. a, Selected drug molecules containing 1,3-difunctionalized cyclobutane skeleton. **b,** Current strategies[50–54] for the synthesis of highly functionalized cyclobutanes via strain release. **c,** Our hypothesis on the 1,3-difunctionalization of BCBs by remote C–H activation to access valuable 1,1,3-trisubstituted and 1,1,3,3-tetrasubstituted cyclobutanes via a Ru-XAT process. Ar, aryl.; Het, heteroarenes.

functionalization; (3) exceedingly mild reaction conditions and (4) outstanding chemo- and site selectivities (Fig. 1c).

Results and discussion

Optimization studies

We initiated our studies on BCBs 1,3-difunctionalization through remote C–H activation, with benzyl-bicyclo[1.1.0]butane-1-carboxylate (**1a**), 2-phenylpyridine (**2a**) and ethyl-2-bromo-2,2-difluoroacetate (**3a**) as the model substrates (Table 1). We were pleased to find that the desired product **4** was efficiently obtained in 75% isolated yield with Ru(O$_2$CMes)$_2$(p-cymene) as the catalyst and P(4-CF$_3$C$_6$H$_4$)$_3$ (Table 1, entry 1). Next, a series of phosphines, as well as alternative ligands such as bipyridine (bpy) and N-heterocyclic carbene (NHC), were tested, and P(4-CF$_3$C$_6$H$_4$)$_3$ was found to be superior (Table 1, entries 2 and 3). Ru(OAc)$_2$(p-cymene) gave the desired product **4** with 52% yield, while [RuCl$_2$(p-cymene)]$_2$ was ineffective (Table 1, entry 4), highlighting the importance of carboxylate assistance in the C–H ruthenation[74]. [Ru(^{t}BuCN)$_5$(H$_2$O)](BF$_4$)$_2$[75] as a precatalyst gave inferior results (Table 1, entry 5). Control experiments revealed the crucial role of the ruthenium catalyst and the phosphine ligand for the BCBs C–C cleavage difunctionalization (Table 1, entry 6).

With the optimized reaction conditions in hand, we subsequently evaluated the viable substrate scope for the bifunctionalization of BCBs **1** with differently substituted heteroarenes **2** (Fig. 2). Arenes with distinct electronic features and substituents, such as fluorine, thioether, bromine, ester and keto groups, were fully tolerated by the versatile catalyst (**5–29**). Transformable pyrazoles, ketimine and oxazolines could be employed to guarantee *meta*-selectivity (**17–24, 30**). Drug-relevant motifs, such as diazepam, purines and nucleoside proved to be viable for the ruthenium-catalysed BCBs difunctionalization (**26–29**).

Table 1 | Optimization of the reaction parameters
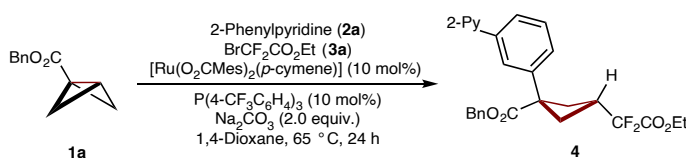
Entry	Variation from the standard conditions[a]	Yield (%)[b]
1	None	75
2	PPh$_3$/P[3,5-(CF$_3$)$_2$C$_6$H$_3$]$_3$/P(4-OMeC$_6$H$_4$)$_3$	54/34/43
3	bpy/NHC as ligand[c]	0/trace
4	[Ru(OAc)$_2$(p-cymene)]/[RuCl$_2$(p-cymene)]$_2$	52/5
5	[Ru(^{t}BuCN)$_5$(H$_2$O)](BF$_4$)$_2$	21[d]/ 30
6	No catalyst/no ligand	0/0

[a]Reaction conditions: **1a** (0.3 mmol), **2a** (3.0 equiv.), **3a** (3.0 equiv.), [Ru] (10 mol%), ligand (10 mol%), Na$_2$CO$_3$ (2.0 equiv.), 1,4-dioxane (2.0 ml), T = 65 °C, t = 24 h. [b]Yield of isolated products. [c]bpy, 2,2'-bipyridine, NHC ligand used 1,3-bis(2,6-diisopropylphenyl)imidazolium chloride. [d]T = 50 °C. Ac, acetyl; Bn, benzyl; Mes, mesityl; 2-Py, 2-pyridyl.

A series of substituted BCB esters **1** furnished the 1,1,3-trisubstituted cyclobutanes **31–37** (Fig. 3). Thus, BCBs featuring sensitive functional groups, including ester, thiophene, ketone, amide and sulfone (**38–41**) were efficiently converted to desired products. Furthermore, disubstituted BCBs were identified as amenable substrates (**42–47**). Here, disubstituted BCBs favoured to form a benzylic radical rather than a tertiary radical, chemo-selectively delivering
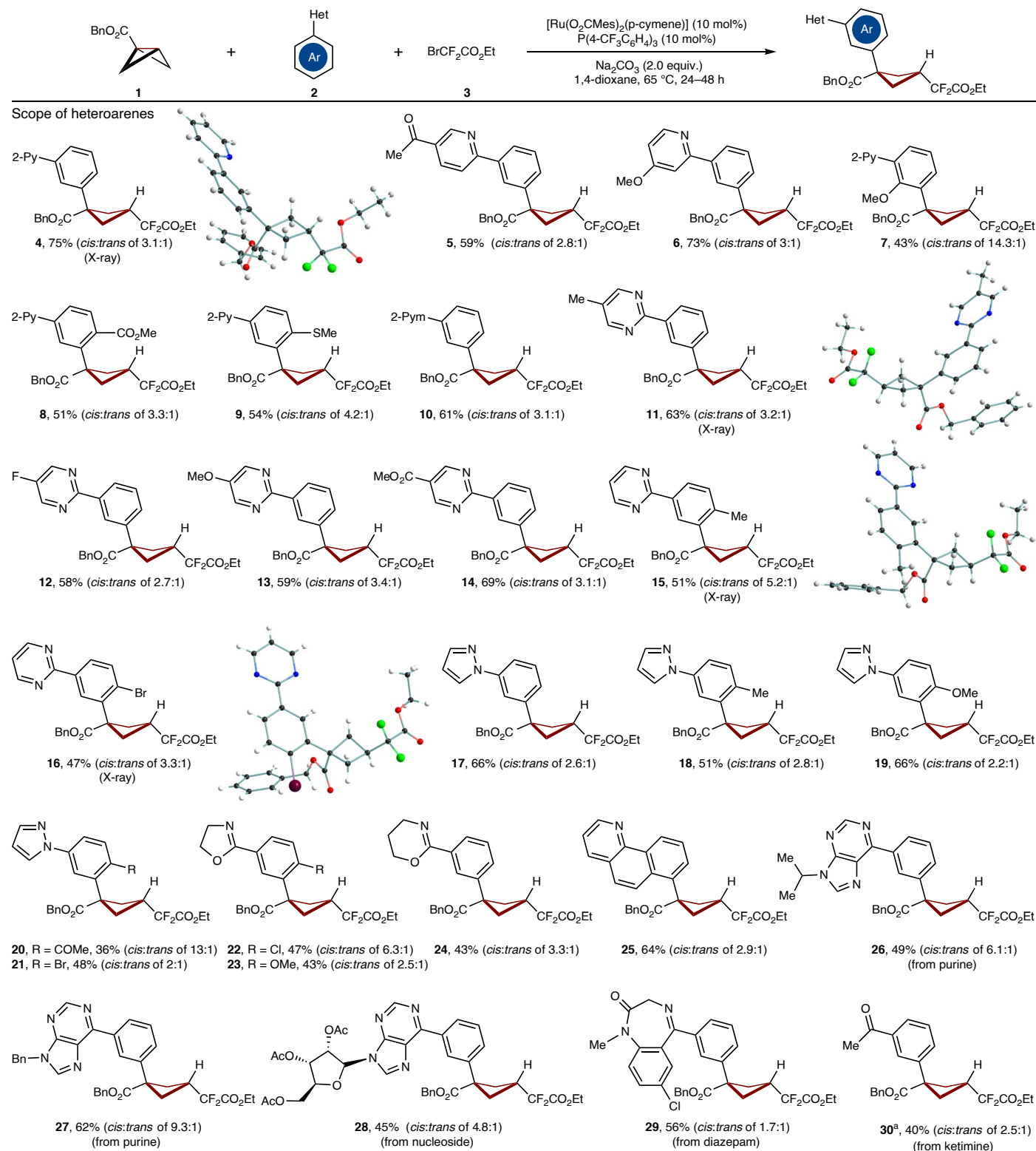
Fig. 2 | Scope of heteroarenes. Reaction conditions: **1** (0.3 mmol), **2** (3.0 equiv.), **3** (3.0 equiv.), [Ru(O$_2$CMes)$_2$(p-cymene)] (10 mol%), P(4-CF$_3$C$_6$H$_4$)$_3$ (10 mol%), Na$_2$CO$_3$ (2.0 equiv.), 1,4-dioxane (2.0 ml), 65 °C, 24–48 h. All yields are isolated yields. The ratios of the diastereomers (*cis* and *trans*) were determined by

^{1}H-NMR spectroscopy or isolated yield. ^{a}Work-up with 3 N HCl and stirring for a further 3 h. Note that the presented structures are the major isomers. Bn, benzyl; Mes, mesityl; Py, pyridyl; Pym, pyrimidinyl.

diarylcyclobutane motifs. Likewise, a wide range of alkyl halides, such as perfluoroalkane halides, fluorine-free alkyl bromide, monofluoroalkyl bromide and difluoroalkyl amides were tolerated to give the desired cyclobutanes **48–57**.

Gram-scale and late-stage derivatization

To demonstrate the practical utility of our BCBs C–C scission/remote activation strategy, cyclobutane **4** was prepared at gram scale with comparable efficacy (Fig. 4a). The site selectivity ensured that
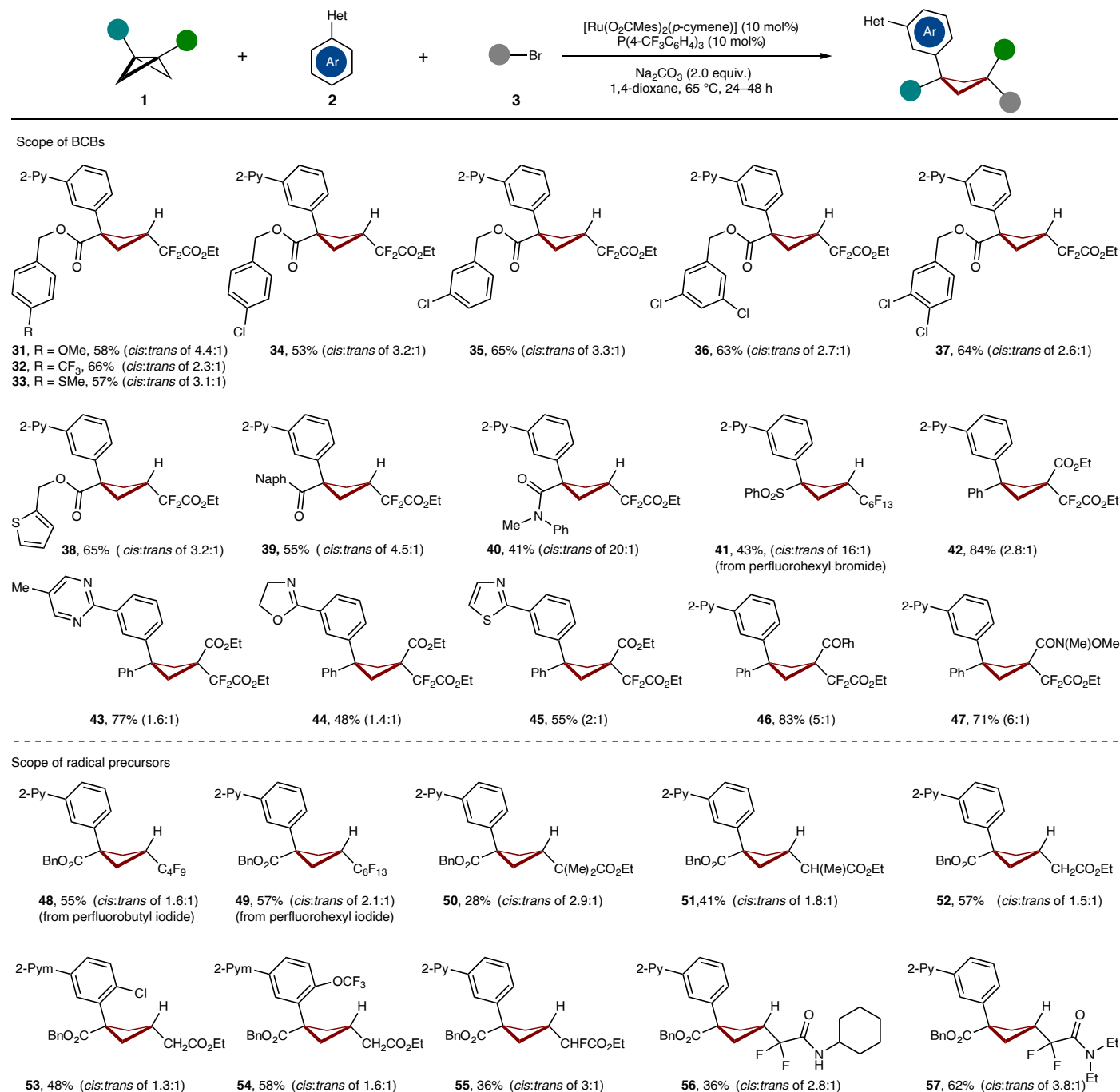
Fig. 3 | Scope of BCBs and radical precursors. Reaction conditions: **1** (0.3 mmol), **2** (3.0 equiv.), **3** (3.0 equiv.), [Ru(O₂CMes)₂(p-cymene)] (10 mol%), P(4-CF₃C₆H₄)₃ (10 mol%), Na₂CO₃ (2.0 equiv.), 1,4-dioxane (2.0 mL), 65 °C, 24–48 h. All yields are isolated yields. The ratios of the diastereomers were determined by ¹H-NMR spectroscopy or isolated yields. Note that the presented structures are the major isomers. In the case of the 1,1,3-trisubstituted cyclobutanes, the *cis* structure is the major, while for the 1,1,3,3-tetrasubstituted cyclobutanes, the (1*r*,3*r*) structure is the major, which was confirmed by X-ray crystallographic analysis (see the X-ray structure of compound **62** in Supplementary Data 6 for details). Naph, 2-naphthyl group.

pyrimidine, oxazoline and ketimine (vide infra) as well as pyridine and pyrazole were efficiently diversified, extending the viable portfolio (Fig. 4b). Further, a triple activation manifold proved viable in terms of ruthenium(II)-catalysed C−C/*meta*-C−H and *ortho*-photo-induced C−H activation (**58** and **59**).

DFT calculation and mechanism studies

To gain insights into the reaction mechanism, the site selectivity of radical addition at the two possible BCB sites was probed by means of density functional theory (DFT) calculations (Fig. 5a; see

Supplementary Figs. 1, 2, 7 and 8 for details). In the case of monosubstituted BCB **1a**, the difluoroalkyl radical preferentially attacked at the unsubstituted carbon, leading to the formation of a more thermodynamically stable tertiary radical. The shorter bridge C−C distance (1.61 Å) and the longer C−C$_{RF}$ distance (2.21 Å) in **TS3-s4**, compared with **TS4-s2**, indicated that the radical attack at the unsubstituted site proceeded through an earlier transition state that structurally resembled the starting BCB **1a**. In the case of radical addition to the disubstituted BCB **1m**, the ester-substituted site is favoured, resulting in the formation of thermodynamically stable benzylic radical.
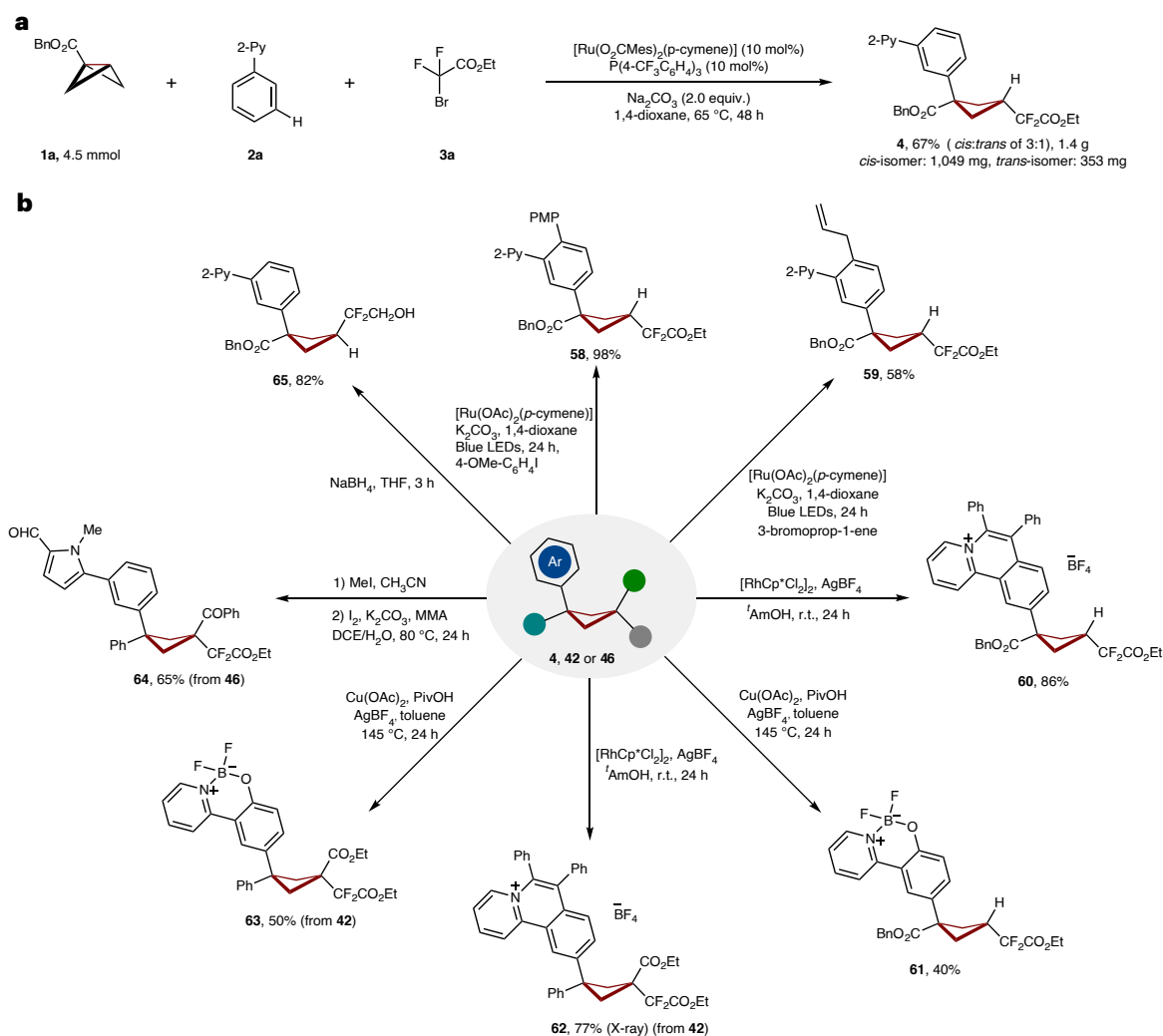
Fig. 4 | Gram-scale and late-stage derivatization. a, Gram-scale reaction gave the desired product **4** in high yield. **b**, Various downstream functionalization of products **4**, **42** or **46**. Cp*, 1,2,3,4,5-pentamethylcyclopentadienyl; DCE, 1,2-dichloroethane; LED, light emitting diode; MMA, methyl methacrylate; Piv, pivaloyl; PMP, *p*-methoxyphenyl; r.t., room temperature; THF, tetrahydrofuran.

During the cleavage of the σ-bridge bond in disubstituted BCB **1m**, **TS7-s1** exhibited an earlier transition state characteristic, evidenced by the slightly elongated C–C bridge distance of BCB **1a** (1.63 Å in **TS7-s1** and 1.64 Å in **TS8-s1**) and the relatively larger C–C distances between the BCB **1m** and the difluoroalkyl radical (2.25 Å in **TS7-s1** and 2.21 Å in **TS8-s1**). The presynthesized *p*-cymene-free ruthenacycle **66** yielded the desired product **4** in the presence of MesCO$_2$H and phosphine ligand (Fig. 5b). The control experiment without a phosphine ligand as well as with alternative ligands, such as bpy or NHC, in the optimization table failed to provide the desired product, highlighting the essential role of the phosphine ligand assistance[76–79]. The key role of the phosphine ligand was further demonstrated by attempting this transformation with carboxylate-free ruthenium(II) phosphine complex **67**, yielding the desired product in high yield when MesCO$_2$H was added (Fig. 5c). The carboxylate-free ruthenium(II) phosphine complex **67** could afford the desired product only in 14% yield even in the absence of MesCO$_2$H (Fig. 5c). Additionally, radical trapping experiments validated the radical mechanism (see Supplementary Data 7.1.1 for details). On the basis of our mechanism and computational findings, a plausible catalytic cycle is put forwards in Fig. 5d, featuring ruthenacycle **A** in a ruthenacycle-mediated XAT process to furnish ruthenium(III) intermediate **B** with an energy barrier of 14.9 kcal mol^{-1}. The thus formed alkyl radical **3^R** attacks the BCB **1a**

at the unsubstituted site to induce strain-release C–C scission with an energy barrier of 15.9 kcal mol^{-1}, forming the tertiary radical **C**. Species **C** reacts at the ruthena(III)cycle **B** *para* to the C$_{Ar}$–Ru bond, delivering the stabilized singlet metallacycle **D**. Here, the formation of the *cis* product is favoured over the *trans* product by 1.4 kcal mol^{-1}. The subsequent rearomatization and proto-demetallation releases the desired cyclobutane **4**, thereby regenerating the catalytically active ruthenium(II) species **F**.

Conclusions

We have achieved the merger of BCBs C–C activation with remote *meta*-C–H functionalization by a multipotent ruthenium catalyst. The double activation proceeded in a highly chemo- and position-selective fashion and provided access to densely decorated F*sp*^{3}-rich cyclobutanes in a single step. Mechanistic studies were suggestive of a Ru-XAT process enabling chemo-selective BCBs opening and *meta*-diversification.

Methods

General methods for 1,3-difunctionalization of BCBs enabled by ruthenium-catalysed remote C–H activation
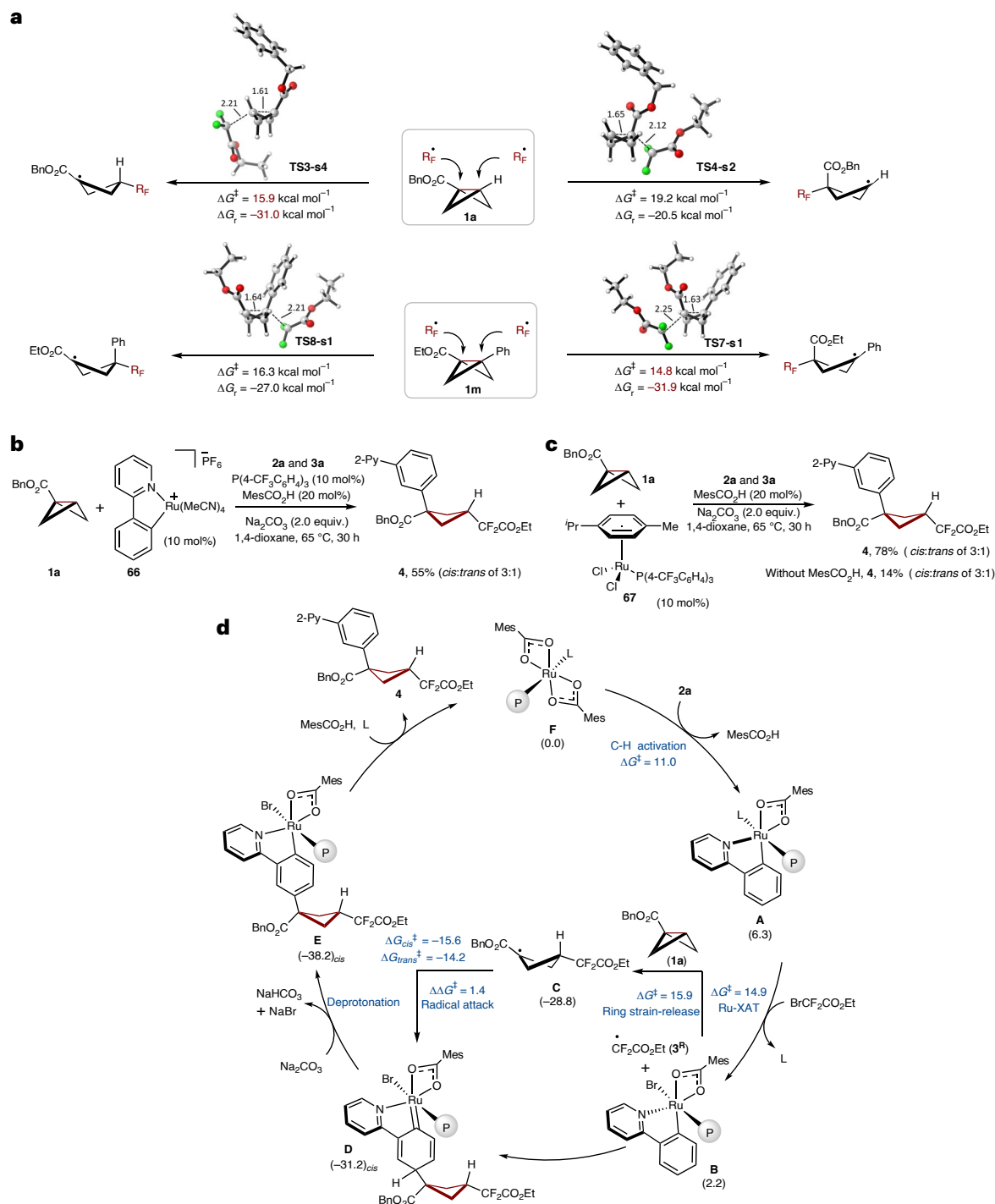The general procedure for 1,3-difunctionalization of BCBs was as follows: [Ru(O$_2$CMes)$_2$(*p*-cymene)] (16.8 mg, 10.0 mol%), P(4-CF$_3$C$_6$H$_4$)$_3$

Fig. 5 | DFT calculation and mechanism studies. a, Computed relative Gibbs free energies ($\Delta G_{338.15}$) in kcal mol^{-1} for radical attack at the monosubstituted BCB **1a** and disubstituted BCB **1m** were conducted at the B3LYP-D3BJ/def2-TZVP-SMD(1,4-dioxane)//PBE0-D3BJ/def2-SVP level of theory. **b**, *p*-Cymene-free ruthenacycle complex **66** as the catalyst. **c**, Carboxylate-free ruthenium(II) phosphine complex **67** as the catalyst. **d**, Proposed catalytic cycle associated with relative Gibbs free energies ($\Delta G_{338.15}$) in kcal mol^{-1} based on our mechanism studies and DFT calculation. RF, difluoroalkyl; P, P(4-CF$_3$C$_6$H$_4$)$_3$; L, 1,4-dioxane, **2a** and so on.

(14.0 mg, 10.0 mol%), Na$_2$CO$_3$ (64 mg, 0.6 mmol, 2.0 equiv.), 1,4-dioxane (2.0 ml), **1** (0.3 mmol, 1.0 equiv.), **2** (0.9 mmol, 3.0 equiv.) and **3** (0.9 mmol, 3.0 equiv.) were added into an oven-dried 20 ml pressure tube. The reaction mixture was stirred at 65 °C for 24–48 h. After cooling to ambient temperature, the mixture was purified by column chromatography on silica gel to afford the corresponding cyclobutanes **4**–**57**.

Data availability

The authors declare that the data supporting the findings of this study are available within the paper and its Supplementary Information files. All other requests for materials and information should be addressed to the corresponding authors. Crystallographic data for the structures reported in this article have been deposited at the Cambridge Crystallographic Data Centre, under deposition numbers CCDC 2344919 (**15**),

2344920 (**11**), 2344921 (**16**), 2344922 (**4**) and 2344923 (**62**). Copies of the data can be obtained free of charge via https://www.ccdc.cam. ac.uk/structures/.

References

1. Lovering, F., Bikker, J. & Humblet, C. Escape from flatland: increasing saturation as an approach to improving clinical success. *J. Med. Chem.* **52**, 6752–6756 (2009).
2. Mykhailiuk, P. K. Saturated bioisosteres of benzene: where to go next? *Org. Biomol. Chem.* **17**, 2839–2849 (2019).
3. Nicolaou, K. C. et al. Synthesis and biopharmaceutical evaluation of imatinib analogues featuring unusual structural motifs. *ChemMedChem* **11**, 31–37 (2016).
4. Golfmann, M. & Walker, J. C. L. Bicyclobutanes as unusual building blocks for complexity generation in organic synthesis. *Commun. Chem.* **6**, 9 (2023).
5. Kelly, C. B., Milligan, J. A., Tilley, L. J. & Sodano, T. M. Bicyclobutanes: from curiosities to versatile reagents and covalent warheads. *Chem. Sci.* **13**, 11721–11737 (2022).
6. Bellotti, P. & Glorius, F. Strain-release photocatalysis. *J. Am. Chem. Soc.* **145**, 20716–20732 (2023).
7. Turkowska, J., Durka, J. & Gryko, D. Strain release—an old tool for new transformations. *Chem. Commun.* **56**, 5718–5734 (2020).
8. Tsien, J. et al. Three-dimensional saturated C(sp^3)-rich bioisosteres for benzene. *Nat. Rev. Chem.* **8**, 605–627 (2024).
9. Bauer, M. R. et al. Put a ring on it: application of small aliphatic rings in medicinal chemistry. *RSC Med. Chem.* **12**, 448–471 (2021).
10. Wager, T. T. et al. Discovery of two clinical histamine H3 receptor antagonists: *trans*-*N*-ethyl-3-fluoro-3-[3-fluoro-4-(pyrrolidinylmethyl)-phenyl]cyclobutanecarboxamide (PF-03654746) and *trans*-3-fluoro-3-[3-fluoro-4-(pyrrolidin-1-ylmethyl)phenyl]-N-(2-methylpropyl)cyclobutanecarboxamide (PF-03654764). *J. Med. Chem.* **54**, 7602–7620 (2011).
11. Warshamana-Greene, G. S. et al. The insulin-like growth factor-I receptor kinase inhibitor, NVP-ADW742, sensitizes small cell lung cancer cell lines to the effects of chemotherapy. *Clin. Cancer Res.* **11**, 1563–1571 (2005).
12. Wrobleski, M. L. et al. Cyclobutane derivatives as potent NK1 selective antagonists. *Bioorg. Med. Chem. Lett.* **16**, 3859–3863 (2006).
13. Mulvihill, M. J. et al. A selective and orally efficacious dual inhibitor of the IGF-1 receptor and insulin receptor. *Future Med. Chem.* **1**, 1153–1171 (2009).
14. Dong, W. et al. Exploiting the sp^2 character of bicyclo[1.1.1] pentyl radicals in the transition-metal-free multi-component difunctionalization of [1.1.1]propellane. *Nat. Chem.* **14**, 1068–1077 (2022).
15. Huang, W., Keess, S. & Molander, G. A. Dicarbofunctionalization of [1.1.1]propellane enabled by nickel/photoredox dual catalysis: one-step multicomponent strategy for the synthesis of BCP-aryl derivatives. *J. Am. Chem. Soc.* **144**, 12961–12969 (2022).
16. Yu, I. F. et al. Catalytic undirected borylation of tertiary C–H bonds in bicyclo[1.1.1]pentanes and bicyclo[2.1.1]hexanes. *Nat. Chem.* **15**, 685–693 (2023).
17. Zhang, X. et al. Copper-mediated synthesis of drug-like bicyclopentanes. *Nature* **580**, 220–226 (2020).
18. Nugent, J. et al. Synthesis of all-carbon disubstituted bicyclo[1.1.1] pentanes by iron-catalyzed Kumada cross-coupling. *Angew. Chem. Int. Ed.* **59**, 11866–11870 (2020).
19. Wang, H. et al. Dearomative ring expansion of thiophenes by bicyclobutane insertion. *Science* **381**, 75–81 (2023).
20. Liang, Y., Nematswerani, R., Daniliuc, C. G. & Glorius, F. Silver-enabled cycloaddition of bicyclobutanes with isocyanides for the synthesis of polysubstituted 3-azabicyclo[3.1.1]heptanes. *Angew. Chem. Int. Ed.* **63**, e202402730 (2024).
21. Denisenko, A. et al. 2-Oxabicyclo[2.1.1]hexanes as saturated bioisosteres of the *ortho*-substituted phenyl ring. *Nat. Chem.* **15**, 1155–1163 (2023).
22. Dhake, K. et al. Beyond bioisosteres: divergent synthesis of azabicyclohexanes and cyclobutenyl amines from bicyclobutanes. *Angew. Chem. Int. Ed.* **61**, e202204719 (2022).
23. Zhang, J., Su, J.-Y., Zheng, H., Li, H. & Deng, W.-P. Eu(OTf)$_3$-catalyzed formal dipolar [4π+2σ] cycloaddition of bicyclo-[1.1.0] butanes with nitrones: access to polysubstituted 2-oxa-3-azabicyclo[3.1.1]heptanes. *Angew. Chem. Int. Ed.* **63**, e202318476 (2024).
24. Yang, Y. et al. Programmable late-stage functionalization of bridge-substituted bicyclo[1.1.1]pentane bis-boronates. *Nat. Chem.* **16**, 285–293 (2024).
25. Yang, Y. et al. An intramolecular coupling approach to alkyl bioisosteres for the synthesis of multisubstituted bicycloalkyl boronates. *Nat. Chem.* **13**, 950–955 (2021).
26. Bychek, R. M. et al. Difluoro-substituted bicyclo[1.1.1]pentanes for medicinal chemistry: design, synthesis, and characterization. *J. Org. Chem.* **84**, 15106–15117 (2019).
27. Agasti, S. et al. A catalytic alkene insertion approach to bicyclo[2.1.1]hexane bioisosteres. *Nat. Chem.* **15**, 535–541 (2023).
28. Kleinmans, R. et al. Intermolecular [2π+2σ]-photocycloaddition enabled by triplet energy transfer. *Nature* **605**, 477–482 (2022).
29. Guo, R. et al. Strain-release [2π+2σ] cycloadditions for the synthesis of bicyclo[2.1.1]hexanes initiated by energy transfer. *J. Am. Chem. Soc.* **144**, 7988–7994 (2022).
30. Zheng, Y. et al. Photochemical intermolecular [3σ+2σ]-cycloaddition for the construction of aminobicyclo[3.1.1]heptanes. *J. Am. Chem. Soc.* **144**, 23685–23690 (2022).
31. Ni, D. et al. Intermolecular formal cycloaddition of indoles with bicyclo[1.1.0]butanes by Lewis acid catalysis. *Angew. Chem. Int. Ed.* **62**, e202308606 (2023).
32. Radhoff, N., Daniliuc, C. G. & Studer, A. Lewis acid catalyzed formal (3+2)-cycloaddition of bicyclo[1.1.0]butanes with ketenes. *Angew. Chem. Int. Ed.* **62**, e20230477 (2023).
33. Dutta, S. et al. Double strain-release [2π+2σ]-photocycloaddition. *J. Am. Chem. Soc.* **146**, 5232–5241 (2024).
34. Dutta, S. et al. Photoredox-enabled dearomative [2π+2σ] cycloaddition of phenols. *J. Am. Chem. Soc.* **146**, 2789–2797 (2024).
35. de Robichon, M. et al. Enantioselective, intermolecular [π2+σ2] photocycloaddition reactions of 2(1*H*)-quinolones and bicyclo[1.1.0] butanes. *J. Am. Chem. Soc.* **145**, 24466–24470 (2023).
36. Tang, L. et al. Silver-catalyzed dearomative [2π+2σ] cycloadditions of indoles with bicyclobutanes: access to indoline fused bicyclo[2.1.1]hexanes. *Angew. Chem. Int. Ed.* **62**, e202310066 (2022).
37. Liu, Y. et al. Pyridine-boryl radical-catalyzed [2π+2σ] cycloaddition of bicyclo[1.1.0]-butanes with alkenes. *ACS Catal.* **13**, 5096–5103 (2023).
38. Nguyen, T. V. T., Bossonnet, A., Wodrich, M. D. & Waser, J. Photocatalyzed [2σ+2σ] and [2σ+2π] cycloadditions for the synthesis of bicyclo[3.1.1]heptanes and 5- or 6-membered carbocycles. *J. Am. Chem. Soc.* **145**, 25411–25421 (2023).
39. Yu, T. et al. Selective [2σ+2σ]-cycloaddition enabled by boronyl radical catalysis: synthesis of highly substituted bicyclo[3.1.1] heptanes. *J. Am. Chem. Soc.* **145**, 4304–4310 (2023).
40. Frank, N. et al. Synthesis of *meta*-substituted arene bioisosteres from [3.1.1]propellane. *Nature* **611**, 721–726 (2022).
41. Iida, T. et al. Practical and facile access to bicyclo[3.1.1]heptanes: potent bioisosteres of *meta*-substituted benzenes. *J. Am. Chem. Soc.* **144**, 21848–21852 (2022).
42. Gianatassio, R. et al. Strain-release amination. *Science* **351**, 241–246 (2016).

43. Lopchuk, J. M. et al. Strain-release heteroatom functionalization: development, scope, and stereospecificity. *J. Am. Chem. Soc.* **139**, 3209–3226 (2017).

44. Ernouf, G., Chirkin, E., Rhyman, L., Ramasami, P. & Cintrat, J. Photochemical strain-release-driven cyclobutylation of C(*sp*³)-centered radicals. *Angew. Chem. Int. Ed.* **59**, 2618–2622 (2020).

45. Ociepa, M., Wierzba, A. J., Turkowska, J. & Gryko, D. Polarity-reversal strategy for the functionalization of electrophilic strained molecules via light-driven cobalt catalysis. *J. Am. Chem. Soc.* **142**, 5355–5361 (2020).

46. Kang, G. et al. Transannular C–H functionalization of cycloalkane carboxylic acids. *Nature* **618**, 519–525 (2023).

47. Fan, Z., Strassfeld, D. A., Park, H. S., Wu, K. & Yu, J.-Q. Formal γ-C–H functionalization of cyclobutyl ketones: synthesis of *cis*-1,3-difunctionalized cyclobutanes. *Angew. Chem. Int. Ed.* **62**, e202303948 (2023).

48. Dasgupta, A. et al. Stereoselective alder-ene reactions of bicyclo[1.1.0]butanes: facile synthesis of cyclopropyl- and aryl-substituted cyclobutenes. *J. Am. Chem. Soc.* **146**, 1196–1203 (2023).

49. Kraemer, Y. et al. Overcoming a radical polarity mismatch in strain-release pentafluorosulfanylation of [1.1.0] bicyclobutanes: an entryway to sulfone- and carbonyl-containing SF₅-cyclobutanes. *Angew. Chem. Int. Ed.* **63**, e202319930 (2024).

50. Silvi, M. & Aggarwal, V. K. Radical addition to strained σ-bonds enables the stereocontrolled synthesis of cyclobutyl boronic esters. *J. Am. Chem. Soc.* **141**, 9511–9515 (2019).

51. Fawcett, A., Biberger, T. & Aggarwal, V. K. Carbopalladation of C–C σ-bonds enabled by strained boronate complexes. *Nat. Chem.* **11**, 117–122 (2019).

52. Bennett, S. H. et al. Difunctionalization of C–C σ-bonds enabled by the reaction of bicyclo[1.1.0]butyl boronate complexes with electrophiles: reaction development, scope, and stereochemical origins. *J. Am. Chem. Soc.* **142**, 16766–16775 (2020).

53. Shen, H.-C. et al. Iridium-catalyzed asymmetric difunctionalization of C–C σ-bonds enabled by ring-strained boronate complexes. *J. Am. Chem. Soc.* **145**, 16508–16516 (2023).

54. Wang, H. et al. *Syn*-selective difunctionalization of bicyclobutanes enabled by photoredox-mediated C–S σ-bond scission. *J. Am. Chem. Soc.* **145**, 23771–23780 (2023).

55. Lusi, R. F., Perea, M. A. & Sarpong, R. C–C bond cleavage of α-pinene derivatives prepared from carvone as a general strategy for complex molecule synthesis. *Acc. Chem. Res.* **55**, 746–758 (2022).

56. Murakami, M. & Ishida, N. Cleavage of carbon–carbon σ-bonds of four-membered rings. *Chem. Rev.* **121**, 264–299 (2021).

57. Sokolova, O. O. & Bower, J. F. Selective carbon–carbon bond cleavage of cyclopropylamine derivatives. *Chem. Rev.* **121**, 80–109 (2021).

58. Nairoukh, Z., Cormier, M. & Marek, I. Merging C–H and C–C bond cleavage in organic synthesis. *Nat. Rev. Chem.* **1**, 0035 (2017).

59. Xu, Y. et al. Deacylative transformations of ketones via aromatization-promoted C–C bond activation. *Nature* **567**, 373–378 (2019).

60. Murphy, S. K., Park, J.-W., Cruz, F. A. & Dong, V. M. Rh-catalyzed C–C bond cleavage by transfer hydroformylation. *Science* **347**, 56–60 (2015).

61. Rogge, T. et al. C–H activation. *Nat. Rev. Methods Primer* **1**, 43 (2021).

62. Leow, D., Li, G., Mei, T.-S. & Yu, J.-Q. Activation of remote *meta*-C–H bonds assisted by an end-on template. *Nature* **486**, 518–522 (2012).

63. Tang, R.-Y., Li, G. & Yu, J.-Q. Conformation-induced remote *meta*-C–H activation of amines. *Nature* **507**, 215–220 (2014).

64. Wang, X. C. et al. Ligand-enabled *meta*-C–H activation using a transient mediator. *Nature* **519**, 334–338 (2015).

65. Shi, H. et al. Enantioselective remote *meta*-C–H arylation and alkylation via a chiral transient mediator. *Nature* **558**, 581–585 (2018).

66. Kuninobu, Y. et al. A *meta*-selective C–H borylation directed by a secondary interaction between ligand and substrate. *Nat. Chem.* **7**, 712–717 (2015).

67. Robbins, D. W. & Hartwig, J. F. Sterically controlled alkylation of arenes through iridium-catalyzed C–H borylation. *Angew. Chem. Int. Ed.* **52**, 933–937 (2013).

68. Ramadoss, B., Jin, Y., Asako, S. & Ilies, L. Remote steric control for undirected *meta*-selective C–H activation of arenes. *Science* **375**, 658–663 (2022).

69. Saidi, O. et al. Ruthenium-catalyzed *meta*-sulfonation of 2-phenylpyridines. *J. Am. Chem. Soc.* **133**, 19298–19301 (2011).

70. Hofmann, N. & Ackermann, L. *meta*-Selective C–H bond alkylation with secondary alkyl halides. *J. Am. Chem. Soc.* **135**, 5877–5884 (2013).

71. Wang, X.-G. et al. Three-component ruthenium-catalyzed direct *meta*-selective C–H activation of arenes: a new approach to the alkylarylation of alkenes. *J. Am. Chem. Soc.* **141**, 13914–13922 (2019).

72. Wang, Y., Chen, S., Chen, X., Zangarelli, A. & Ackermann, L. Photo-induced ruthenium-catalyzed double remote C(*sp*²)–H/C(*sp*³)–H functionalizations by radical relay. *Angew. Chem. Int. Ed.* **61**, e202205562 (2022).

73. Chen, S., Yuan, B., Wang, Y. & Ackermann, L. Ruthenium-catalyzed remote difunctionalization of nonactivated alkenes for double *meta*-C(*sp*²)–H/C-6(*sp*³)–H functionalization. *Angew. Chem. Int. Ed.* **62**, e202301168 (2023).

74. Ackermann, L. Carboxylate-assisted transition-metal-catalyzed C–H bond functionalizations: mechanism and scope. *Chem. Rev.* **111**, 1315–1345 (2011).

75. McArthur, G. et al. An air- and moisture-stable ruthenium precatalyst for diverse reactivity. *Nat. Chem.* https://doi.org/10.1038/s41557-024-01481-5 (2024).

76. Neogi, S. et al. Silylarylation of alkenes via *meta*-selective C–H activation of arenes under ruthenium/iron cooperative catalysis: mechanistic insights from combined experimental and computational studies. *ACS Catal.* **14**, 4510–4522 (2024).

77. Ruan, Z. et al. Ruthenium(II)-catalyzed *meta* C–H mono- and difluoromethylations by phosphine/carboxylate cooperation. *Angew. Chem. Int. Ed.* **56**, 2045–2049 (2017).

78. Gou, X. Y. et al. Ruthenium-catalyzed radical cyclization/*meta*-selective C–H alkylation of arenes via σ-activation strategy. *ACS Catal.* **11**, 4263–4270 (2021).

79. Guillemard, L., Ackermann, L. & Johansson, M. J. Late-stage *meta*-C–H alkylation of pharmaceuticals to modulate biological properties and expedite molecular optimisation in a single step. *Nat. Commun.* **15**, 3349 (2024).

Acknowledgements

Author contributions

L.A. conceived the project. S.C. designed the experiments and performed initial screening studies. S.C., Z.X. and X.-Y.G. performed synthetic experiments. B.Y. carried out DFT theoretical studies. S.C., B.Y. and L.A. wrote the paper. L.A. supervised the project.

Funding

Competing interests

The authors declare no competing interests.

Additional information